



Fluid flow in the osteocyte mechanical environment: a fluid-structure interaction approach

Title	Fluid flow in the osteocyte mechanical environment: a fluid-structure interaction approach
Author(s)	Verbruggen, Stefaan W.;Vaughan, Ted J.;McNamara, Laoise M.
Publication Date	2013-04-09
Publisher	Springer Verlag
Repository DOI	10.1007/s10237-013-0487-y

1 **Fluid Flow in the Osteocyte Mechanical Environment:**

2 **A Fluid-Structure Interaction Approach**

3 Stefaan W. Verbruggen, Ted J. Vaughan, Laoise M. McNamara

4 Biomechanics Research Centre (BMEC), Mechanical and Biomedical Engineering,

5 College of Engineering and Informatics,

6 National University of Ireland, Galway

7
8 Address for correspondence:

9 Dr. Laoise M. McNamara

10 Department of Mechanical and Biomedical Engineering

11 National University of Ireland Galway

12 Galway,

13 Ireland

14 Phone: (353) 91-492251

15 Fax: (353) 91-563991

16 Email: Laoise.McNamara@nuigalway.ie

17
18 Key words of the paper: Bone, osteocyte, mechanobiology, lacuna, fluid-structure interaction, shear
19 stress

20

ABSTRACT

1
2 Osteocytes are believed to be the primary sensor of mechanical stimuli in bone, which
3 orchestrate osteoblasts and osteoclasts to adapt bone structure and composition to meet
4 physiological loading demands. Experimental studies to quantify the mechanical environment
5 surrounding bone cells are challenging and as such computational and theoretical approaches
6 have modelled either the solid or fluid environment of osteocytes to predict how these cells
7 are stimulated in vivo. Osteocytes are an elastic cellular structure that deforms in response to
8 the external fluid flow imposed by mechanical loading. This represents a most challenging
9 multi-physics problem in which fluid and solid domains interact and as such no previous
10 study has accounted for this complex behaviour. The objective of this study is to employ
11 fluid-structure interaction (FSI) modelling to investigate the complex mechanical
12 environment of osteocytes in vivo. Fluorescent staining of osteocytes was performed in order
13 to visualize their native environment and develop geometrically accurate models of the
14 osteocyte in vivo. By simulating loading levels representative of vigorous physiological
15 activity (3,000 $\mu\epsilon$ compression and 300 Pa pressure gradient), we predict average interstitial
16 fluid velocities ($\sim 60.5 \mu\text{m/s}$) and average maximum shear stresses ($\sim 11 \text{ Pa}$) surrounding
17 osteocytes in vivo. Interestingly these values occur in the canaliculi around the osteocyte cell
18 processes and are within the range of stimuli known to stimulate osteogenic responses by
19 osteoblastic cells in vitro. Significantly our results suggest that the greatest mechanical
20 stimulation of the osteocyte occurs in the cell processes, which cell culture studies have
21 indicated is the most mechanosensitive area of the cell. These are the first computational FSI
22 models to simulate the complex multi-physics mechanical environment of osteocyte in vivo
23 and provide a deeper understanding of bone mechanobiology.

1 **1. INTRODUCTION**

2 Bone is a highly efficient material, capable of remodelling its mass and structure in
3 response to everyday mechanical loading. This adaptive behaviour is believed to be
4 orchestrated by osteocyte cells, which recruit osteoblasts and osteoclasts to adapt bone
5 structure and composition in response to changes in physiological loading. In vitro cell
6 culture studies have suggested that osteoblasts and osteocytes act as sensors of mechanical
7 stimuli in bone (Owan et al. 1997; Smalt et al. 1997), but that osteocytes are the most
8 sensitive bone cell type to mechanical stimulation (Ajubi et al. 1996; Klein-Nulend et al.
9 1995; Westbroek et al. 2000), and also the most influential for stimulating osteogenesis
10 (Birmingham et al. 2012b).

11 The precise mechanical stimuli that osteocytes experience in vivo has been much debated.
12 Experimental studies point to loading-induced fluid flow around the osteocyte as the primary
13 stimulus for bone growth (Owan et al. 1997; Smalt et al. 1997; You et al. 2000). Theoretical
14 studies have predicted that loading the bone matrix surrounding osteocytes generates a
15 pressure differential that drives flow of interstitial fluid within the lacunar-canalicular
16 network (Weinbaum et al. 1994; Han et al. 2004; Wang et al. 2005; Wang et al. 2007; You et
17 al. 2001). The fluid flow generates a shear stress on the osteocyte cell membrane and this is
18 thought to act as a stimulus for biochemical signalling (Knothe Tate and Knothe 2000;
19 Knothe Tate et al. 1998a; Knothe Tate et al. 1998b; Knothe Tate et al. 2000; Wang et al.
20 2000), a theory substantiated by experimental observations of bone cells responding to flow
21 derived shear stress and not streaming potentials or chemotransport (Bakker et al. 2001). In
22 vitro cell culture studies, in which osteoblastic cells were exposed to various mechanical
23 stimuli, have suggested that load-induced interstitial fluid flow may stimulate a stronger
24 osteogenic response than direct mechanical strain in bone cells (Owan et al. 1997; Smalt et al.
25 1997; You et al. 2000). Recent in vitro studies have observed osteogenic responses in

1 osteocyte-like cells exposed to fluid shear stress levels between 0.4 and 1.2 Pa within in vitro
2 flow experiments (Bacabac et al. 2004; Bakker et al. 2001), while previous studies have
3 similarly shown a bone growth response in cells exposed to substrate strains greater than
4 10,000 $\mu\epsilon$ (Burger and Veldhuijzen 1993; You et al. 2000). Furthermore mechanical
5 stimulation has been shown to enhance bone tissue regeneration in vitro to a certain extent
6 (Sittichokechaiwut et al. 2009). However, existing tissue regeneration approaches do not
7 strive to mimic the in vivo mechanical environment surrounding cells, primarily because
8 these stimuli are unknown. It is likely that mechanobiology based approaches for bone tissue
9 regeneration would be enhanced if levels of mechanical stimulation applied to cells in vitro
10 were analogous to those experienced in vivo during bone growth. Therefore characterisation
11 of the mechanical stimulus experienced by osteocytes within the lacunar-canalicular network
12 is necessary.

13 As osteocytes are embedded in a mineralised extracellular matrix, direct experimental
14 studies are challenging. Researchers have sought to overcome this problem by developing
15 mathematical and analytical models of interstitial fluid flow in bone. Initially bone was
16 treated as a biphasic continuum, with the application of Biot's poroelastic theory (Biot 1941;
17 Biot 1955), and these studies predicted that pressure gradients resulting from mechanical
18 loading generated fluid flow around the osteocyte (Piekarski and Munro 1977). Analytical
19 models of idealised osteocyte canaliculi under load-induced fluid flow have been developed
20 and applied to predict the in vivo range for shear stress (0.8-3 Pa) and deformation of
21 osteocyte cell membranes (Han et al. 2004; Weinbaum et al. 1994; You et al. 2001; Zeng et
22 al. 1994). Recent analytical models have suggested that interstitial fluid viscosity and
23 pericellular matrix permeability are the dominant parameters affecting flow in the lacunar-
24 canalicular network (Sansalone et al. 2012). Computational finite element modelling
25 techniques have also been applied to idealised models of the lacunar-canalicular system and

1 have predicted abrupt changes in the drag forces within the canaliculi arising from changes in
2 geometry or proximity to bone microporosity and the Haversian canals (Mak et al. 1997).
3 One study investigated the fluid environment of an idealised osteocyte and predicted high
4 shear stresses within the canaliculi whereas the osteocyte cell body is primarily exposed to
5 hydrodynamic pressure (Anderson et al. 2005). Recent studies identified projections of the
6 extracellular matrix into the pericellular space around the canaliculi (McNamara et al. 2009),
7 and theoretical and computational studies have suggested that such projections amplify the
8 strain stimulus to the osteocyte (Han et al. 2004; Verbruggen et al. 2012; Anderson and
9 Knothe Tate 2008). Ultra high voltage electron microscopes (UHVEM) have been used to
10 develop highly detailed computational models of 80 nm long sections of osteocyte canaliculi
11 of canaliculi, and these have been applied to predict that the geometry of the pericellular
12 space greatly affects the velocity of fluid flow around the osteocyte cell processes (Kamioka
13 et al. 2012).

14 In all previous computational models bone cells and tissue were modelled using either
15 solid mechanics approaches (where extracellular fluids were modelled using poroelastic
16 assumptions) or fluid dynamics modelling, wherein the biological tissues were assumed to be
17 rigid for the purposes of understanding fluid flow and shear stresses. In reality, bone cells are
18 composed of an elastic cell membrane that deforms in response to the external fluid flow
19 imposed by mechanical loading (Knothe Tate 2003). The assumption that osteocytes are
20 static rigid bodies precludes the elucidation of cellular strains arising from fluid flow in the
21 lacunar canalicular network (Anderson et al. 2005; Anderson and Knothe Tate 2008;
22 Kamioka et al. 2012). To fully simulate this behaviour represents a most challenging multi-
23 physics problem, which is too complex to solve analytically and requires a fluid-structure
24 interaction (FSI) approach.

1 Furthermore previous studies have used idealised geometries (Anderson et al. 2005; Rath
2 Bonivitch et al. 2007) or have modelled limited portions of the cell (Anderson and Knothe
3 Tate 2008), but computational models have recently shown that the use of idealised
4 geometries predicts stress and strain values which are significantly lower than those predicted
5 by geometries developed from physiological imaging (Anderson and Knothe Tate 2008;
6 Verbruggen et al. 2012). In vitro experimental studies have shown that the geometry of the
7 bone cell affects its response to strain (Bacabac et al. 2008). Therefore an approach which
8 examines the effect of the complex architecture of the lacunar-canalicular network on fluid
9 shear stress and cellular strains in osteocytes is required.

10 The objective of this research is to use computational methods to predict the mechanical
11 environment of osteocytes in vivo under physiological loading. Using representative models
12 of the osteocyte and its environment with fluid structure interaction (FSI) techniques we
13 examine both shear stresses on the cell membrane and resulting strain within the osteocyte
14 arising from mechanically-driven interstitial fluid flow in vivo.

15

16

17

18

19

20

1 **2. MATERIALS AND METHODS**

2 **2.1. Model generation**

3 Fluorescent staining of thick transverse sections of the mid-diaphysis of the tibia of a
4 male 6-8 month old Sprague-Dawley rat was performed, using FITC (Fluorescein
5 Isothiocyanate isomer I, Sigma-Aldrich) solution at 1 per cent in ethanol to visualize the
6 pericellular space (Verbruggen et al. 2012). Confocal scanning of osteocytes was performed
7 using a confocal microscope (Zeiss LSM 51) with a 40x oil immersion lens at laser
8 wavelength excitation of 488 nm, allowing visualisation of their native environment.
9 Confocal microscopy allowed acquisition of a z-stack of scans through the depth of the
10 sample, taken at 2048 x 2048 x 47 pixels with a field of view of 255 μm , resulting in a
11 resolution of 0.1 μm in x-y plane and 0.6 μm in the z axis, that were then used to develop
12 geometrically accurate models of osteocytes as previously described (Verbruggen et al.
13 2012). Briefly, MIMICS (Materialise) image processing software was used to generate 3D
14 reconstructions of the images, with thresholding to between -884 and -769 Hounsfield units
15 to allow segmentation of the lacunar-canalicular space from the surrounding matrix
16 (Verbruggen et al. 2012). These models were then meshed using 3-Matic (Materialise) voxel-
17 meshing software to create four solid osteocyte models with anatomically accurate
18 geometries (Verbruggen et al. 2012). Boolean operations were applied to generate a
19 surrounding extracellular matrix (ECM) and pericellular fluid space (PCS), offset from the
20 osteocyte model by 0.08 μm , based on experimental measurements of the geometry of the
21 osteocyte environment (McNamara et al. 2009; Wang et al. 2005; You et al. 2004). These
22 models were meshed with ANSYS SOLID72 tetrahedral elements and exported to ANSYS.
23 Models of an idealised osteocyte and an idealised osteocyte with ECM projections were
24 generated to compare with the representative geometries (Verbruggen et al. 2012), similar to

1 the methods described above. The four representative geometries and the idealised geometry
2 are shown in Fig. 1 (A-D) and Fig. 1 (E) respectively.

3 **2.2. Fluid-structure interaction analyses:**

4 **2.2.1. *Solid Material and Fluid Properties***

5 All solid structures were modelled as linearly elastic, isotropic materials. An elastic
6 modulus of 16 GPa and Poisson's ratio of 0.38 was attributed to the ECM (Deligianni and
7 Apostolopoulos 2008). A modulus of 4.47 kPa and Poisson's ratio of 0.3 was attributed to the
8 osteocyte cell body and processes (Sugawara et al. 2008).

9 The properties of the interstitial fluid were assumed to be similar to salt water, with a
10 density of 997 kgm^{-3} and a dynamic viscosity of $0.000855 \text{ kgm}^{-1}\text{s}^{-1}$ (Anderson et al. 2005).
11 Flow within the lacunar-canalicular system was assumed to be laminar in nature.

12 **2.2.2. *Boundary conditions and loading***

13 Two-way fluid-structure simulations were conducted using coupled ANSYS Multi-
14 physics software to investigate the behaviour of interstitial fluid under physiological
15 conditions. Two levels of fluid-solid interactions are performed to simulate interaction
16 between the ECM and the interstitial fluid and also between this fluid and the osteocyte cell
17 membrane.

18 The initial two-way FSI simulation is conducted through a bi-directional coupling of the
19 ANSYS CFX solver to the ANSYS Structural finite element (FE) solver. A displacement
20 boundary condition was applied to model faces to generate a compressive load of $3,000 \mu\text{e}$,
21 representative of vigorous physiological loading (Burr et al. 1996). Due to the fact that
22 mechanical loading in bone occurs on the whole organ level, with compression and tension
23 occurring in different regions driving fluid across the bone network, a pressure gradient is

1 applied across the models to represent this (Knothe Tate 2003; Manfredini et al. 1999; Steck
2 et al. 2003; Knothe Tate and Niederer 1998). Therefore an inlet pressure of 300 Pa was
3 assigned to the inlets on one face and the remaining inlets were defined as outlets at a relative
4 pressure of 0 Pa (Manfredini et al. 1999; Steck et al. 2003; Knothe Tate and Niederer 1998),
5 similar to the pressure gradient applied by Anderson et al. (Anderson et al. 2005).

6 While in vivo loading of bone is dynamic and cyclic (Fritton et al. 2000), the linear
7 elastic material properties used here allowed simplification of loading to ramped static
8 loading. Loading was applied uni-axially and symmetrically, to represent longitudinal
9 compression of long bones in vivo (Taylor et al. 1996), with opposing faces constrained
10 symmetrically to prevent rigid body motion. Using a staggered iteration approach inherent in
11 ANSYS coupling software, the deformations at the interface between the ECM and the PCS
12 resulting from the applied loading are mapped onto the fluid domain. The resulting fluid
13 equations are solved and forces are relayed back to the solid ECM domain as new boundary
14 conditions, allowing gradual mesh motion and strongly coupled solution through further
15 iterations. This staggered iteration approach is performed repeatedly within each step until
16 convergence of the field equations and a fully implicit solution is achieved. Upon solution of
17 this FSI analysis, the loading-induced fluid flow can be analysed. The pressure load on the
18 cell membrane arising from the flow is then exported to ANSYS Structural and interpolated
19 onto the surface of the solid osteocyte domain. This FSI analysis facilitates investigation of
20 the deformation and strain in the cell generated by the interstitial fluid boundary conditions
21 imposed by global matrix loading.

22

23

24

1

2 **3. RESULTS**

3 The complex multi-physics nature of this study allows analysis of multiple aspects of the
4 osteocyte mechanical environment, which are examined in sequence here.

5 **3.1. Interstitial fluid velocity:**

6 The streamline plots in Fig. 2B and Fig. 3 show the velocity distribution on the surface of
7 representative osteocytes. Qualitatively it can be seen from these images that regions of
8 highest velocities are located within osteocyte canaliculi, with maximum velocities of 238.1-
9 325.7 $\mu\text{m/s}$ ($\sigma = 298.48 \pm 35.84 \mu\text{m/s}$) in representative models and 219.2 $\mu\text{m/s}$ in the
10 idealised model. In contrast fluid velocities were much lower surrounding the osteocyte cell
11 body, with magnitudes of approximately 38-79 $\mu\text{m/s}$ ($\sigma = 60.58 \pm 16.5 \mu\text{m/s}$) predicted in the
12 representative models and approximately 27 $\mu\text{m/s}$ observed in the idealised models (see Fig.
13 7A). It can also be seen that the fluid velocity within canaliculi is affected by variations in
14 surface roughness of the canalicular wall. This is noticeable in the effect of ECM projections
15 on fluid flow in the osteocyte canaliculi as shown in Fig. 6. Fluid velocity is seen to increase
16 in these areas in both the representative and idealised osteocytes (Fig. 6A and 6C).

17 **3.2. Shear stress on the cell membrane:**

18 The shear stress distribution on the surface of the representative osteocytes resulting from
19 the interstitial fluid flow is shown in Fig. 2C and Fig. 4. Visually the highest shear stresses
20 are predicted within the osteocyte canaliculi, resulting in stress concentrations on the cell
21 processes (see Fig. 6B). A similar effect is seen in idealised models when ECM projections
22 are included (see Fig. 6D). Maximum shear stresses are shown in Fig. 7B, and are observed
23 to increase to 6.9 Pa in the idealised models with the inclusion of ECM projections in the
24 osteocyte canaliculi. The representative models experience even higher levels of shear stress

1 stimulus, with maximum shear stresses of approximately 9.5-15.2 Pa ($\sigma = 11.6 \pm 2.5$ Pa)
2 located in the canaliculi. All osteocyte models experienced shear stress above the level of
3 shear stress required for bone growth (0.8 Pa) (Han et al. 2004; Weinbaum et al. 1994; You et
4 al. 2001; Zeng et al. 1994), with the amount of the cell membrane stimulated to this level
5 shown in Fig. 8A.

6 **3.3. Strain within the osteocyte:**

7 The strain experienced in the representative osteocyte cell membranes is visible in the
8 contour plots in Fig. 2D and Fig. 5. The strain distribution in the representative and idealised
9 osteocytes is shown in Fig. 8B. While cellular strains greater than 10,000 $\mu\epsilon$ were predicted
10 in discrete areas of the models most of the cell membranes, approximately 81-98% ($\sigma = 90.1$
11 $\pm 6.1\%$) were strained by less than 1,000 $\mu\epsilon$.

12

13

14

15

16

17

18

19

20

21

1 4. DISCUSSION

2 This study develops the first fluid-structure interaction models to investigate the complex
3 interaction between the solid and fluid phases within the osteocyte environment in vivo.
4 These models simulate interstitial fluid flow arising from mechanical deformation of the bone
5 matrix and pressure gradients under loading conditions representative of vigorous physical
6 activity. This study allows the investigation of the velocities of the interstitial fluid, the shear
7 stress imparted onto the surface of the cell and the resulting strain in the osteocyte cell
8 processes and body. Such findings predict the mechanical stimuli to osteocytes under loading
9 conditions known to stimulate an osteogenic response.

10 The modelling of a complex mechanical environment such as the lacunar-canalicular
11 network necessitates a number of assumptions. The resolution of the images used to generate
12 the models (0.1 μm), is amongst the highest obtainable on commercially available confocal
13 microscopes. As the diameter of the canaliculus is ~ 100 nm, the most highly fluorescent
14 canaliculi are more easily discernible and less fluorescent canaliculi are omitted during
15 thresholding operations, resulting in fewer processes than exist in vivo. Although
16 transmission electron microscopy (TEM) resolutions could overcome this issue, obtaining the
17 full 3D information of an osteocyte through serial TEM is unfeasible due to the small size of
18 ultrathin slices required (~ 9 nm) relative to the size of an osteocyte environment (~ 50 μm). It
19 must be noted that, as the greatest stimulation in our models occurs in the canaliculi, we
20 expect that inclusion of more canaliculi, as are present in vivo, would result in even greater
21 stimulation of the osteocyte at these levels of loading.

22 For the purposes of this study the ECM and osteocyte materials were assumed to be linear
23 elastic isotropic materials, with cell properties assigned from values observed in cultured
24 bone cells (Sugawara et al. 2008) and the mesh-like pericellular matrix was not included. The
25 viscoelastic nature of the cell was neglected as physiological loading of bones occurs at a
26 frequency of approximately 1 Hz, well below the relaxation time of 41.5 s measured in bone

1 cells (Appelman et al. 2011; Darling et al. 2008). Furthermore the inherent anisotropy of the
2 cell was neglected in this study in order to focus on the multi-physics effects of loading-
3 induced fluid flow. However we have investigated the effect of transverse isotropy previously
4 through a finite element approach and reported 3.7-12.2% greater strain transfer to the
5 osteocyte when compared to isotropic cells (Verbruggen et al. 2012). Thus the stimulation
6 predicted in the current study would be enhanced with the inclusion of an active actin
7 cytoskeleton, which has been shown to result in higher reaction forces and increased tension
8 inside the cells (Dowling et al. 2012; McGarry 2009; McGarry et al. 2009; Ofek et al. 2010;
9 Ronan et al. 2012). As the fluid dynamics of the interstitial fluid are not well understood,
10 laminar uni-directional flow was assumed based on studies of the nano-scale dimensions of
11 the canalicular channels (Anderson et al. 2005; Cheng and Giordano 2002). Realistically
12 dynamic flow and cyclic loading conditions occur in vivo, and experimental studies suggest
13 that shear strain rate on the cell membrane is an important mechanical factor in bone
14 mechanobiology (Bacabac et al. 2004; Fritton et al. 2000; Goldstein et al. 1991; Lanyon and
15 Rubin 1984). The incorporation of dynamic physiological boundary conditions in future
16 studies, along with an active actin cytoskeleton, would further amplify the stimulus observed
17 in this study and provide more realistic simulations of osteocyte mechanobiology in vivo.

18 Mechanical loading in bone occurs on the whole organ level, with compression and
19 tension occurring on opposite regions in the bone. This global loading generates a much
20 higher pressure gradient than across the region of a single cell, driving fluid from one side of
21 the organ to the other and resulting in gradients as large as the 300 Pa gradient applied in this
22 study (Manfredini et al. 1999; Steck et al. 2003). A recent computational study has predicted
23 pressure gradients within individual canaliculi as high as 1 Pa/nm, the equivalent of an
24 approximately 800 Pa pressure gradient along the length of a single canaliculus (Kamioka et
25 al. 2012). While we have represented this global loading as a localised pressure gradient in

1 this study we anticipate that an anatomically accurate lacunar-canalicular network, employing
2 a multi-scale modelling approach to derive the boundary conditions across multiple scales
3 (Vaughan et al. 2012), may elucidate the pressure gradient induced across individual
4 osteocytes.

5 While previous researchers have employed CFD techniques to predict fluid flow in the
6 lacunar-canalicular system (Anderson et al. 2005; Anderson and Knothe Tate 2008; Kamioka
7 et al. 2012), this study provides the first investigation of the effect of bone matrix
8 deformation on flow of interstitial fluid, and subsequent deformation of the osteocyte cell
9 membranes in a fully three-dimensional anatomically-accurate osteocyte environment. While
10 FSI modelling has recently been applied to model individual cells under in vitro conditions
11 (Vaughan et al. 2013) and to investigate the mechanics of the bone marrow cavity
12 (Birmingham et al. 2012a), these techniques have not yet been applied to the in vivo
13 environment of individual bone cells. We report here that average velocities of approximately
14 $60.5 \mu\text{m/s}$ occur within the pericellular space, which are similar to those observed in
15 experimental fluorescein tracer studies ($\sim 60 \mu\text{m/s}$) (Price et al. 2011).

16 Examination of the strain distribution in the osteocyte resulting from loading-induced
17 fluid flow shows that strain levels are much lower than $10,000 \mu\epsilon$, which in vitro substrate
18 strain studies have shown is required to stimulate osteoblast and osteocyte activity (Burger
19 and Veldhuijzen 1993; You et al. 2000). Indeed most of the cell volumes (81-98%)
20 experience strains below $1,000 \mu\epsilon$, an order of magnitude lower than that required for an
21 osteogenic response. This implies that mechanically-driven fluid flow alone in the canalicular
22 system is not sufficient to generate a strain-related osteogenic response. In a previous study
23 we predicted strain stimuli of $23\text{-}26,000 \mu\epsilon$ by a solid mechanics finite element approach
24 using these representative models, assuming that the PCM was a solid continuum
25 (Verbruggen et al. 2012). This glycocalyx matrix has been shown to reduce permeability by

1 an order of magnitude (Anderson et al. 2008), resisting flow and inducing strain in the
2 osteocyte cell membrane (Goulet et al. 2009; Gururaja et al. 2005; Sansalone et al. 2012).
3 Thus the inclusion of such a matrix would likely reduce the magnitudes of fluid velocity and
4 the resulting shear stresses. However the presence of tethering elements in the PCM would
5 also likely result in an increase in strain transfer to the osteocyte predicted here, as has been
6 demonstrated analytically (Han et al. 2004; Wang et al. 2007; You et al. 2001; Zeng et al.
7 1994). The models in the current study do not include tethering elements as these are too
8 small (~0.5 μm long) to be accurately captured at confocal resolutions, while serial TEM
9 imaging of an entire osteocyte with tethering elements would prove extremely challenging
10 due to the small size (~9 nm) of ultrathin sections required relative to the size on an osteocyte
11 environment (~50 μm). We propose that the absence of these tethers of the peri-cellular
12 matrix accounts for the low strain values predicted along the osteocyte membrane.

13 There has been much debate within the osteocyte community as to whether the stimulus
14 to the osteocyte is amplified through tethering elements (Han et al. 2004) or through ECM
15 projections that disturb the flow or attach directly to the cell processes (Anderson and Knothe
16 Tate 2008; Verbruggen et al. 2012; Wang et al. 2007). While tethering elements have not
17 been included in this study, our results do show that variations in the canalicular geometry,
18 particularly the ECM projections, act as shear stress stimulus amplifiers in the osteocyte
19 geometry, similar to previous computational fluid dynamics (CFD) studies (Anderson and
20 Knothe Tate 2008).

21 These projections have been shown to contact the cell process (Kamioka et al. 2012;
22 McNamara et al. 2009) and also co-localize with areas of $\beta 3$ integrin staining (McNamara et
23 al. 2009). $\beta 3$ integrin is a key protein in $\alpha V\beta 3$ focal adhesions which have been implicated in
24 matrix invasive and attachment processes (Chatterjee and Chatterjee 2001; Huang et al. 2000)
25 between bone surfaces and osteoclasts (Clover et al. 1992; Engleman et al. 1997; Horton et

1 al. 1991). Additionally, osteopontin is a $\beta 3$ ligand (Horton et al. 1991; Ross et al. 1993),
2 which is present in abundance along the canalicular wall (Devoll et al. 1997; McKee and
3 Nanci 1996; Noda et al. 2003; Sodek and McKee 2000). This evidence strongly suggests that
4 these punctate represent a form of focal adhesion between the osteocyte and the canalicular
5 wall. These attachments would result in both increased strain transfer from the ECM to the
6 osteocyte (Verbruggen et al. 2012; Wang et al. 2007), and increased shear stress stimulus to
7 the osteocyte through disrupted fluid flow as seen previously (Anderson and Knothe Tate
8 2008) and predicted in the current study.

9 The shear stimuli predicted here fall within the range of 0.1-2.2 Pa, which has been
10 shown in cell culture studies of osteoblastic cells to result in increased nitric oxide (NO),
11 prostaglandin (PGE_2) and osteopontin production, biochemicals known to play a key role in
12 the osteogenic (bone forming) response of osteoblasts (Bacabac et al. 2004; Bakker et al.
13 2001; Owan et al. 1997; Smalt et al. 1997). Furthermore in vitro studies have also shown
14 increases in intracellular calcium (Ca^{2+}), an important bone mechanotransduction signalling
15 factor, at shear stress levels of 2 Pa (You et al. 2000). Therefore our findings suggest that
16 under global loading conditions representative of vigorous activity (3000 $\mu\epsilon$), the individual
17 osteocyte is sufficiently stimulated to produce biochemical signals for bone formation.

18 Interestingly our results predict shear stresses on the cell processes in all models that are
19 within the range of 0.8-3 Pa predicted analytically to occur in vivo (Han et al. 2004;
20 Weinbaum et al. 1994; You et al. 2001; Zeng et al. 1994), and are similar to values (~5 Pa)
21 suggested by tracer studies (Price et al. 2011). Our study predicts highly variable fluid
22 velocities and shear stresses within the canaliculi, with inhomogeneous flow patterns
23 occurring similar to those recently predicted using detailed fluid mechanics models of
24 individual canaliculi (Kamioka et al. 2012). However our study predicts that both the

1 maximum velocities and highest shear stress levels were predicted to occur within the
2 canaliculi, and that such stimuli were not predicted surrounding the cell body. Furthermore it
3 was found that the inclusion of ECM projections along the wall of the canaliculi in idealised
4 models resulted in an increase of 152% in shear stress stimulus to the cell. These stimuli were
5 further amplified around these localised projections in representative osteocytes, with
6 increases of 203-300% experienced. This is in agreement with previous finite element and
7 fluid mechanics studies which found that the geometry of the canaliculi can greatly affect the
8 stimulus experienced by the osteocyte cell process (Anderson et al. 2005; Anderson and
9 Knothe Tate 2008; Kamioka et al. 2012; Verbruggen et al. 2012). The current study
10 corroborates this evidence showing that under physiological loading conditions,
11 representative of the in vivo multi-physics environment, interstitial fluid velocities and shear
12 stresses that are both significantly greater in the canaliculi than around the osteocyte cell
13 body. Furthermore, this is the first computational study to explore the effects of both the
14 complex interplay between fluid and solid mechanics and the intricate architecture of the
15 lacunar-canalicular network on osteocyte mechanobiology.

16 The mechanical stimulation within canaliculi is particularly interesting as focal adhesion
17 complexes are localised in osteocytic processes (Kamioka et al. 2006; McNamara et al. 2009;
18 Vatsa et al. 2008) and have been predicted to cause strain concentrations on osteocyte
19 processes by analytical and fluid mechanics modelling approaches (Verbruggen et al. 2012;
20 Wang et al. 2007). Previous cell culture studies have shown that the cell process contains
21 more concentrated and highly organised actin filaments (Tanaka-Kamioka et al. 1998), and
22 for these reasons the cell process is believed to be the most mechanosensitive area of the
23 osteocyte (Adachi et al. 2009). Our findings show that the canaliculus is a more mechanically
24 active region of the lacunar-canalicular network than the lacuna, with the cell processes
25 exposed to the greatest velocities and shear stimuli. Therefore these findings support the

1 hypothesis that osteocyte cell processes in the canaliculi play an important role in osteocyte
2 mechanobiology (Adachi et al. 2009).

3

4

5

6

7

8

9

10

11

12

13

14

15

16

17

18

19

20

21

22

23

24

1 **5. CONCLUSIONS**

2 In this study we report that fluid-structure interaction models of the osteocyte mechanical
3 environment under global loading conditions representative of vigorous activity predict
4 maximum shear stress (~11 Pa) stimulus and average fluid velocities (~60.5 $\mu\text{m/s}$) at the
5 level of the individual osteocyte. Furthermore we observe that the highest stimuli occur in the
6 canaliculi about the osteocytic process, reinforcing the theory that this is the most
7 mechanically active and mechanosensitive region of the osteocyte. These are the first
8 computational models to simulate the complex multi-physics mechanical environment of the
9 osteocyte in vivo and to incorporate the complex 3D lacunar-canalicular architecture,
10 providing a deeper understanding of osteocyte mechanobiology.

11

12 **6. ACKNOWLEDGMENTS**

13 The authors would like to acknowledge funding from the Irish Research Council for Science,
14 Engineering and Technology (IRCSET), under the EMBARK program (S. W. V.), the
15 European Research Council (ERC) under grant number 258992 (BONEMECHBIO) and the
16 Irish Centre for High-End Computing (ICHEC).

17

18

19

20

21

22

23

24

25

1 7. REFERENCES

- 2 Adachi T, Aonuma Y, Tanaka M, Hojo M, Takano-Yamamoto T, Kamioka H (2009)
3 Calcium response in single osteocytes to locally applied mechanical stimulus:
4 Differences in cell process and cell body. *Journal of Biomechanics* 42 (12):1989-1995
- 5 Ajubi NE, Klein-Nulend J, Nijweide PJ, Vrijheid-Lammers T, Alblas MJ, Burger EH (1996)
6 Pulsating Fluid Flow Increases Prostaglandin Production by Cultured Chicken
7 Osteocytes—A Cytoskeleton-Dependent Process. *Biochemical and Biophysical*
8 *Research Communications* 225 (1):62-68. doi:10.1006/bbrc.1996.1131
- 9 Anderson E, Kaliyamoorthy S, Alexander J, Tate M (2005) Nano–Microscale Models of
10 Periosteocytic Flow Show Differences in Stresses Imparted to Cell Body and
11 Processes. *Annals of Biomedical Engineering* 33 (1):52-62. doi:10.1007/s10439-005-
12 8962-y
- 13 Anderson E, Kreuzer S, Small O, Knothe Tate M (2008) Pairing computational and scaled
14 physical models to determine permeability as a measure of cellular communication in
15 micro- and nano-scale pericellular spaces. *Microfluid Nanofluid* 4 (3):193-204.
16 doi:10.1007/s10404-007-0156-5
- 17 Anderson EJ, Knothe Tate ML (2008) Idealization of pericellular fluid space geometry and
18 dimension results in a profound underprediction of nano-microscale stresses imparted
19 by fluid drag on osteocytes. *Journal of Biomechanics* 41 (8):1736-1746
- 20 Appelman TP, Mizrahi J, Seliktar D (2011) A Finite Element Model of Cell-Matrix
21 Interactions to Study the Differential Effect of Scaffold Composition on
22 Chondrogenic Response to Mechanical Stimulation. *Journal of Biomechanical*
23 *Engineering* 133 (4):041010-041012

- 1 Bacabac RG, Mizuno D, Schmidt CF, MacKintosh FC, Van Loon JJWA, Klein-Nulend J,
2 Smit TH (2008) Round versus flat: Bone cell morphology, elasticity, and
3 mechanosensing. *Journal of Biomechanics* 41 (7):1590-1598
- 4 Bacabac RG, Smit TH, Mullender MG, Dijcks SJ, Van Loon JJWA, Klein-Nulend J (2004)
5 Nitric oxide production by bone cells is fluid shear stress rate dependent. *Biochemical
6 and Biophysical Research Communications* 315 (4):823-829
- 7 Bakker AD, Soejima K, Klein-Nulend J, Burger EH (2001) The production of nitric oxide
8 and prostaglandin E2 by primary bone cells is shear stress dependent. *Journal of
9 Biomechanics* 34 (5):671-677
- 10 Biot MA (1941) General Theory of Three-Dimensional Consolidation. *Journal of
11 Applied Physics* 12 (2):155-164. doi:10.1063/1.1712886
- 12 Biot MA (1955) Theory of Elasticity and Consolidation for a Porous Anisotropic Solid.
13 *Journal of Applied Physics* 26 (2):182-185. doi:10.1063/1.1721956
- 14 Birmingham E, Grogan JA, Niebur GL, McNamara LM, McHugh PE (2012a) Computational
15 Modelling of the Mechanics of Trabecular Bone and Marrow Using Fluid Structure
16 Interaction Techniques. *Annals of Biomedical Engineering*:1-13. doi:10.1007/s10439-
17 012-0714-1
- 18 Birmingham E, Niebur GL, McHugh PE, Shaw G, Barry FP, McNamara LM (2012b)
19 Osteogenic differentiation of mesenchymal stem cells is regulated by osteocyte and
20 osteoblast cells in a simplified bone niche. *Eur Cell Mater* 23:13-27. doi:vol023a02
21 [pii]
- 22 Burger EH, Veldhuijzen JP (1993) Influence of mechanical factors on bone formation,
23 resorption and growth in vitro. *Bone* 7:37-56

- 1 Burr DB, Milgrom C, Fyhrie D, Forwood M, Nyska M, Finestone A, Hoshaw S, Saiag E,
2 Simkin A (1996) In vivo measurement of human tibial strains during vigorous
3 activity. *Bone* 18 (5):405-410
- 4 Chatterjee N, Chatterjee A (2001) Role of alphavbeta3 integrin receptor in the invasive
5 potential of human cervical cancer (SiHa) cells. *Journal of environmental pathology,*
6 *toxicology and oncology : official organ of the International Society for*
7 *Environmental Toxicology and Cancer* 20 (3):211-221
- 8 Cheng JT, Giordano N (2002) Fluid flow through nanometer-scale channels. *Physical Review*
9 *E* 65 (3):031206
- 10 Clover J, Dodds RA, Gowen M (1992) Integrin subunit expression by human osteoblasts and
11 osteoclasts in situ and in culture. *Journal of Cell Science* 103 (1):267-271
- 12 Darling EM, Topel M, Zauscher S, Vail TP, Guilak F (2008) Viscoelastic properties of
13 human mesenchymally-derived stem cells and primary osteoblasts, chondrocytes, and
14 adipocytes. *Journal of Biomechanics* 41 (2):454-464
- 15 Deligianni D, Apostolopoulos C (2008) Multilevel finite element modeling for the prediction
16 of local cellular deformation in bone. *Biomechanics and Modeling in*
17 *Mechanobiology* 7 (2):151-159. doi:10.1007/s10237-007-0082-1
- 18 Devoll RE, Pinero GJ, Appelbaum ER, Dul E, Troncoso P, Butler WT, Farach-Carson MC
19 (1997) Improved Immunohistochemical Staining of Osteopontin (OPN) in Paraffin-
20 Embedded Archival Bone Specimens Following Antigen Retrieval: Anti-Human OPN
21 Antibody Recognizes Multiple Molecular Forms. *Calcif Tissue Int* 60 (4):380-386.
22 doi:10.1007/s002239900247
- 23 Dowling EP, Ronan W, Ofek G, Deshpande VS, McMeeking RM, Athanasiou KA, McGarry
24 JP (2012) The effect of remodelling and contractility of the actin cytoskeleton on the

1 shear resistance of single cells: a computational and experimental investigation.
2 Journal of The Royal Society Interface. doi:10.1098/rsif.2012.0428

3 Engleman VW, Nickols GA, Ross FP, Horton MA, Griggs DW, Settle SL, Ruminski PG,
4 Teitelbaum SL (1997) A peptidomimetic antagonist of the alpha(v)beta3 integrin
5 inhibits bone resorption in vitro and prevents osteoporosis in vivo. J Clin Invest 99
6 (9):2284-2292. doi:10.1172/JCI119404

7 Fritton SP, J. McLeod K, Rubin CT (2000) Quantifying the strain history of bone: spatial
8 uniformity and self-similarity of low-magnitude strains. Journal of Biomechanics 33
9 (3):317-325

10 Goldstein SA, Matthews LS, Kuhn JL, Hollister SJ (1991) Trabecular bone remodeling: An
11 experimental model. Journal of Biomechanics 24, Supplement 1 (0):135-150

12 Goulet G, Coombe D, Martinuzzi R, Zernicke R (2009) Poroelastic Evaluation of Fluid
13 Movement Through the Lacunocanalicular System. Annals of Biomedical
14 Engineering 37 (7):1390-1402. doi:10.1007/s10439-009-9706-1

15 Gururaja S, Kim H, Swan C, Brand R, Lakes R (2005) Modeling Deformation-Induced Fluid
16 Flow in Cortical Bone's Canalicular-Lacunar System. Annals of Biomedical
17 Engineering 33 (1):7-25. doi:10.1007/s10439-005-8959-6

18 Han Y, Cowin SC, Schaffler MB, Weinbaum S (2004) Mechanotransduction and strain
19 amplification in osteocyte cell processes. Proceedings of the National Academy of
20 Sciences of the United States of America 101 (47):16689-16694.
21 doi:10.1073/pnas.0407429101

22 Horton MA, Taylor ML, Arnett TR, Helfrich MH (1991) Arg-Gly-Asp (RGD) peptides and
23 the anti-vitronectin receptor antibody 23C6 inhibit dentine resorption and cell
24 spreading by osteoclasts. Experimental Cell Research 195 (2):368-375.
25 doi:[http://dx.doi.org/10.1016/0014-4827\(91\)90386-9](http://dx.doi.org/10.1016/0014-4827(91)90386-9)

1 Huang S, Stupack D, Liu A, Cheresch D, Nemerow GR (2000) Cell growth and matrix
2 invasion of EBV-immortalized human B lymphocytes is regulated by expression of
3 alpha(v) integrins. *Oncogene* 19 (15):1915-1923

4 Kamioka H, Kameo Y, Imai Y, Bakker AD, Bacabac RG, Yamada N, Takaoka A, Yamashiro
5 T, Adachi T, Klein-Nulend J (2012) Microscale fluid flow analysis in a human
6 osteocyte canaliculus using a realistic high-resolution image-based three-dimensional
7 model. *Integrative Biology*

8 Kamioka H, Sugawara Y, Murshid SA, Ishihara Y, Honjo T, Takano-Yamamoto T (2006)
9 Fluid Shear Stress Induces Less Calcium Response in a Single Primary Osteocyte
10 Than in a Single Osteoblast: Implication of Different Focal Adhesion Formation.
11 *Journal of Bone and Mineral Research* 21 (7):1012-1021. doi:10.1359/jbmr.060408

12 Klein-Nulend J, van der Plas A, Semeins CM, Ajubi NE, Frangos JA, Nijweide PJ, Burger
13 EH (1995) Sensitivity of osteocytes to biomechanical stress in vitro. *The FASEB*
14 *Journal* 9 (5):441-445

15 Knothe Tate ML (2003) "Whither flows the fluid in bone?" An osteocyte's perspective.
16 *Journal of Biomechanics* 36 (10):1409-1424

17 Knothe Tate ML, Knothe U (2000) An ex vivo model to study transport processes and fluid
18 flow in loaded bone. *Journal of Biomechanics* 33 (2):247-254. doi:10.1016/s0021-
19 9290(99)00143-8

20 Knothe Tate ML, Knothe U, Niederer P (1998a) Experimental Elucidation of Mechanical
21 Load-Induced Fluid Flow and Its Potential Role in Bone Metabolism and Functional
22 Adaptation. *The American Journal of the Medical Sciences* 316 (3):189-195

23 Knothe Tate ML, Niederer P (1998) A theoretical FE-base model developed to predict the
24 relative contribution of convective and diffusive transport mechanisms for the

1 maintenance of local equilibria within cortical bone. Paper presented at the Advances
2 in Heat and Mass Transfer in Biotechnology, Anaheim, California,

3 Knothe Tate ML, Niederer P, Knothe U (1998b) In Vivo Tracer Transport Through the
4 Lacunocanalicular System of Rat Bone in an Environment Devoid of Mechanical
5 Loading. *Bone* 22 (2):107-117. doi:10.1016/s8756-3282(97)00234-2

6 Knothe Tate ML, Steck R, Forwood MR, Niederer P (2000) In vivo demonstration of load-
7 induced fluid flow in the rat tibia and its potential implications for processes
8 associated with functional adaptation. *Journal of Experimental Biology* 203
9 (18):2737-2745

10 Lanyon LE, Rubin CT (1984) Static vs dynamic loads as an influence on bone remodelling.
11 *Journal of Biomechanics* 17 (12):897-905

12 Mak AFT, Huang DT, Zhang JD, Tong P (1997) Deformation-induced hierarchical flows and
13 drag forces in bone canaliculi and matrix microporosity. *Journal of Biomechanics* 30
14 (1):11-18

15 Manfredini P, Cocchetti G, Maier G, Redaelli A, Montevocchi FM (1999) Poroelastic finite
16 element analysis of a bone specimen under cyclic loading. *Journal of Biomechanics*
17 32 (2):135-144

18 McGarry J (2009) Characterization of Cell Mechanical Properties by Computational
19 Modeling of Parallel Plate Compression. *Annals of Biomedical Engineering* 37
20 (11):2317-2325. doi:10.1007/s10439-009-9772-4

21 McGarry JP, Fu J, Yang MT, Chen CS, McMeeking RM, Evans AG, Deshpande VS (2009)
22 Simulation of the contractile response of cells on an array of micro-posts.
23 *Philosophical Transactions of the Royal Society A: Mathematical,*
24 *Physical and Engineering Sciences* 367 (1902):3477-3497.
25 doi:10.1098/rsta.2009.0097

- 1 McKee MD, Nanci A (1996) Osteopontin at mineralized tissue interfaces in bone, teeth, and
2 osseointegrated implants: Ultrastructural distribution and implications for mineralized
3 tissue formation, turnover, and repair. *Microscopy Research and Technique* 33
4 (2):141-164. doi:10.1002/(sici)1097-0029(19960201)33:2<141::aid-jemt5>3.0.co;2-w
- 5 McNamara LM, Majeska RJ, Weinbaum S, Friedrich V, Schaffler MB (2009) Attachment of
6 Osteocyte Cell Processes to the Bone Matrix. *The Anatomical Record: Advances in*
7 *Integrative Anatomy and Evolutionary Biology* 292 (3):355-363.
8 doi:10.1002/ar.20869
- 9 Noda M, Tsuji K, Nifuji A (2003) Osteopontin: a topic from the point of bone morphology.
10 *Clinical calcium* 13 (4):464-466
- 11 Ofek G, Dowling E, Raphael R, McGarry J, Athanasiou K (2010) Biomechanics of single
12 chondrocytes under direct shear. *Biomechanics and Modeling in Mechanobiology* 9
13 (2):153-162. doi:10.1007/s10237-009-0166-1
- 14 Owan I, Burr DB, Turner CH, Qiu J, Tu Y, Onyia JE, Duncan RL (1997)
15 Mechanotransduction in bone: osteoblasts are more responsive to fluid forces than
16 mechanical strain. *American Journal of Physiology - Cell Physiology* 273 (3):C810-
17 C815
- 18 Piekarski K, Munro M (1977) Transport mechanism operating between blood supply and
19 osteocytes in long bones. *Nature* 269 (5623):80-82
- 20 Price C, Zhou X, Li W, Wang L (2011) Real-time measurement of solute transport within the
21 lacunar-canalicular system of mechanically loaded bone: Direct evidence for load-
22 induced fluid flow. *Journal of Bone and Mineral Research* 26 (2):277-285.
23 doi:10.1002/jbmr.211

- 1 Rath Bonivitch A, Bonewald LF, Nicolella DP (2007) Tissue strain amplification at the
2 osteocyte lacuna: A microstructural finite element analysis. *Journal of Biomechanics*
3 40 (10):2199-2206. doi:10.1016/j.jbiomech.2006.10.040
- 4 Ronan W, Deshpande VS, McMeeking RM, McGarry JP (2012) Numerical investigation of
5 the active role of the actin cytoskeleton in the compression resistance of cells. *Journal*
6 *of the Mechanical Behavior of Biomedical Materials* 14 (0):143-157.
7 doi:10.1016/j.jmbbm.2012.05.016
- 8 Ross FP, Chappel J, Alvarez JI, Sander D, Butler WT, Farach-Carson MC, Mintz KA, Robey
9 PG, Teitelbaum SL, Cheresch DA (1993) Interactions between the bone matrix
10 proteins osteopontin and bone sialoprotein and the osteoclast integrin alpha v beta 3
11 potentiate bone resorption. *Journal of Biological Chemistry* 268 (13):9901-9907
- 12 Sansalone V, Kaiser J, Naili S, Lemaire T (2012) Interstitial fluid flow within bone canaliculi
13 and electro-chemo-mechanical features of the canalicular milieu. *Biomechanics and*
14 *Modeling in Mechanobiology*:1-21. doi:10.1007/s10237-012-0422-7
- 15 Sittichokechaiwut A, Scutt AM, Ryan AJ, Bonewald LF, Reilly GC (2009) Use of rapidly
16 mineralising osteoblasts and short periods of mechanical loading to accelerate matrix
17 maturation in 3D scaffolds. *Bone* 44 (5):822-829. doi:S8756-3282(09)00004-0 [pii]
18 10.1016/j.bone.2008.12.027
- 19 Smalt R, Mitchell FT, Howard RL, Chambers TJ (1997) Induction of NO and prostaglandin
20 E2 in osteoblasts by wall-shear stress but not mechanical strain. *American Journal of*
21 *Physiology - Endocrinology And Metabolism* 273 (4):E751-E758
- 22 Sodek J, McKee MD (2000) Molecular and cellular biology of alveolar bone. *Periodontology*
23 2000 24 (1):99-126. doi:10.1034/j.1600-0757.2000.2240106.x

1 Steck R, Niederer P, Knothe Tate ML (2003) A Finite Element Analysis for the Prediction of
2 Load-induced Fluid Flow and Mechanochemical Transduction in Bone. *Journal of*
3 *Theoretical Biology* 220 (2):249-259

4 Sugawara Y, Ando R, Kamioka H, Ishihara Y, Murshid SA, Hashimoto K, Kataoka N,
5 Tsujioka K, Kajiya F, Yamashiro T, Takano-Yamamoto T (2008) The alteration of a
6 mechanical property of bone cells during the process of changing from osteoblasts to
7 osteocytes. *Bone* 43 (1):19-24

8 Tanaka-Kamioka K, Kamioka H, Ris H, Lim S-S (1998) Osteocyte Shape Is Dependent on
9 Actin Filaments and Osteocyte Processes Are Unique Actin-Rich Projections. *Journal*
10 *of Bone and Mineral Research* 13 (10):1555-1568. doi:10.1359/jbmr.1998.13.10.1555

11 Taylor ME, Tanner KE, Freeman MAR, Yettram AL (1996) Stress and strain distribution
12 within the intact femur: compression or bending? *Medical Engineering & Physics* 18
13 (2):122-131. doi:[http://dx.doi.org/10.1016/1350-4533\(95\)00031-3](http://dx.doi.org/10.1016/1350-4533(95)00031-3)

14 Vatsa A, Semeins CM, Smit TH, Klein-Nulend J (2008) Paxillin localisation in osteocytes—
15 Is it determined by the direction of loading? *Biochemical and Biophysical Research*
16 *Communications* 377 (4):1019-1024. doi:10.1016/j.bbrc.2007.12.174

17 Vaughan TJ, Haugh MG, McNamara LM (2013) A fluid–structure interaction model to
18 characterize bone cell stimulation in parallel-plate flow chamber systems. *Journal of*
19 *The Royal Society Interface* 10 (81). doi:10.1098/rsif.2012.0900

20 Vaughan TJ, McCarthy CT, McNamara LM (2012) A three-scale finite element investigation
21 into the effects of tissue mineralisation and lamellar organisation in human cortical
22 and trabecular bone. *Journal of the Mechanical Behavior of Biomedical Materials* 12
23 (0):50-62

- 1 Verbruggen SW, Vaughan TJ, McNamara LM (2012) Strain amplification in bone
2 mechanobiology: a computational investigation of the in vivo mechanics of
3 osteocytes. *Journal of The Royal Society Interface*. doi:10.1098/rsif.2012.0286
- 4 Wang L, Cowin SC, Weinbaum S, Fritton SP (2000) Modeling Tracer Transport in an Osteon
5 under Cyclic Loading. *Annals of Biomedical Engineering* 28 (10):1200-1209.
6 doi:10.1114/1.1317531
- 7 Wang L, Wang Y, Han Y, Henderson SC, Majeska RJ, Weinbaum S, Schaffler MB (2005) In
8 situ measurement of solute transport in the bone lacunar-canalicular system.
9 *Proceedings of the National Academy of Sciences of the United States of America*
10 102 (33):11911-11916. doi:10.1073/pnas.0505193102
- 11 Wang Y, McNamara LM, Schaffler MB, Weinbaum S (2007) A model for the role of
12 integrins in flow induced mechanotransduction in osteocytes. *Proceedings of the*
13 *National Academy of Sciences* 104 (40):15941-15946. doi:10.1073/pnas.0707246104
- 14 Weinbaum S, Cowin SC, Zeng Y (1994) A model for the excitation of osteocytes by
15 mechanical loading-induced bone fluid shear stresses. *Journal of Biomechanics* 27
16 (3):339-360
- 17 Westbroek I, Ajubi NE, Alblas MJ, Semeins CM, Klein-Nulend J, Burger EH, Nijweide PJ
18 (2000) Differential Stimulation of Prostaglandin G/H Synthase-2 in Osteocytes and
19 Other Osteogenic Cells by Pulsating Fluid Flow. *Biochemical and Biophysical*
20 *Research Communications* 268 (2):414-419. doi:10.1006/bbrc.2000.2154
- 21 You J, Yellowley CE, Donahue HJ, Zhang Y, Chen Q, Jacobs CR (2000) Substrate
22 Deformation Levels Associated With Routine Physical Activity Are Less Stimulatory
23 to Bone Cells Relative to Loading-Induced Oscillatory Fluid Flow. *Journal of*
24 *Biomechanical Engineering* 122 (4):387-393

1 You L-D, Weinbaum S, Cowin SC, Schaffler MB (2004) Ultrastructure of the osteocyte
2 process and its pericellular matrix. *The Anatomical Record Part A: Discoveries in*
3 *Molecular, Cellular, and Evolutionary Biology* 278A (2):505-513.
4 doi:10.1002/ar.a.20050

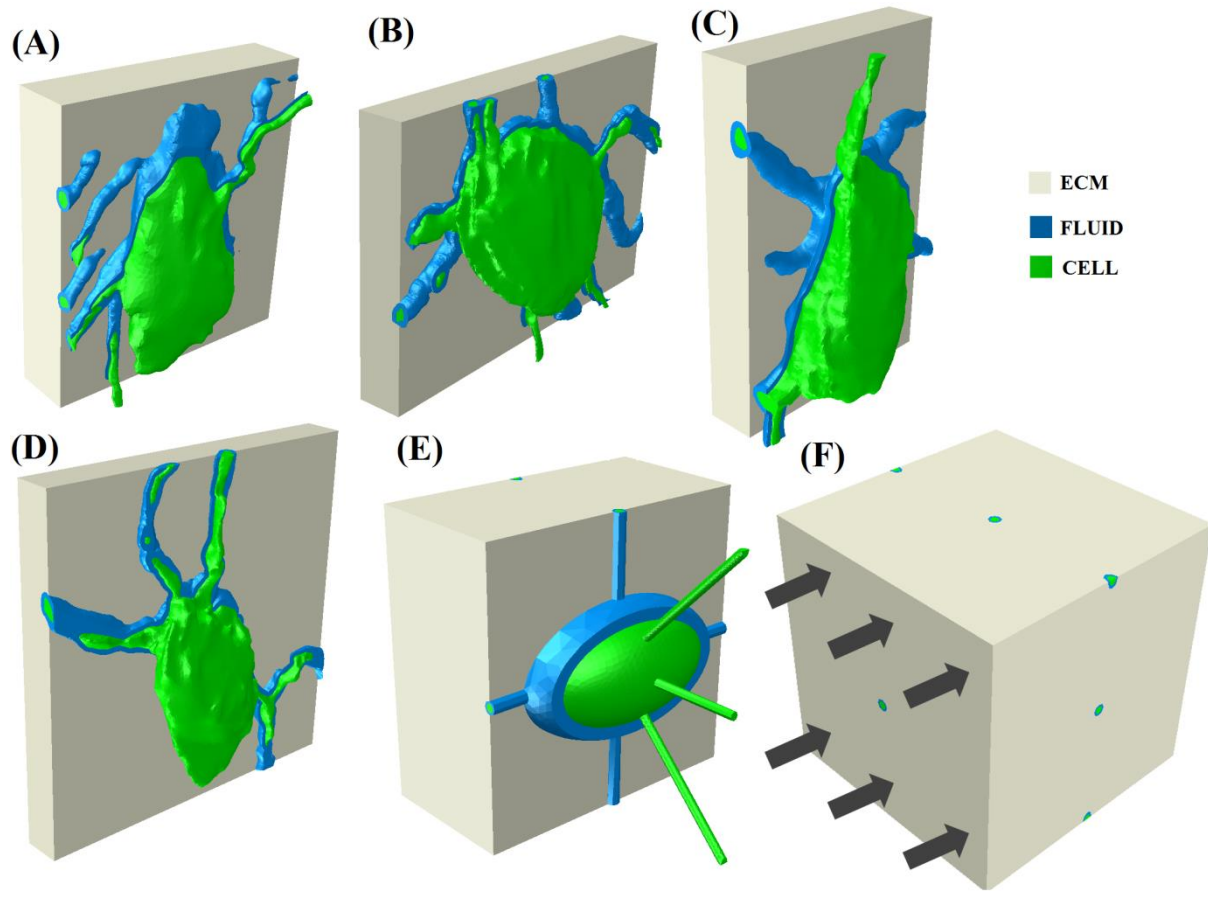
5 You L, Cowin SC, Schaffler MB, Weinbaum S (2001) A model for strain amplification in the
6 actin cytoskeleton of osteocytes due to fluid drag on pericellular matrix. *Journal of*
7 *Biomechanics* 34 (11):1375-1386

8 Zeng Y, Cowin S, Weinbaum S (1994) A fiber matrix model for fluid flow and streaming
9 potentials in the canaliculi of an osteon. *Annals of Biomedical Engineering* 22
10 (3):280-292. doi:10.1007/bf02368235

11

12

13



1

2 **Fig. 1** Composite images of the three components of the representative models (A-D) and the
 3 idealised model (E). The face on which loading and inlet pressure conditions are applied is
 4 also shown (F). In each model the solid extracellular bone matrix (grey) is cut back to reveal
 5 the fluid-filled pericellular space (blue), which is in turn cut back to reveal the solid osteocyte
 6 beneath (green).

7

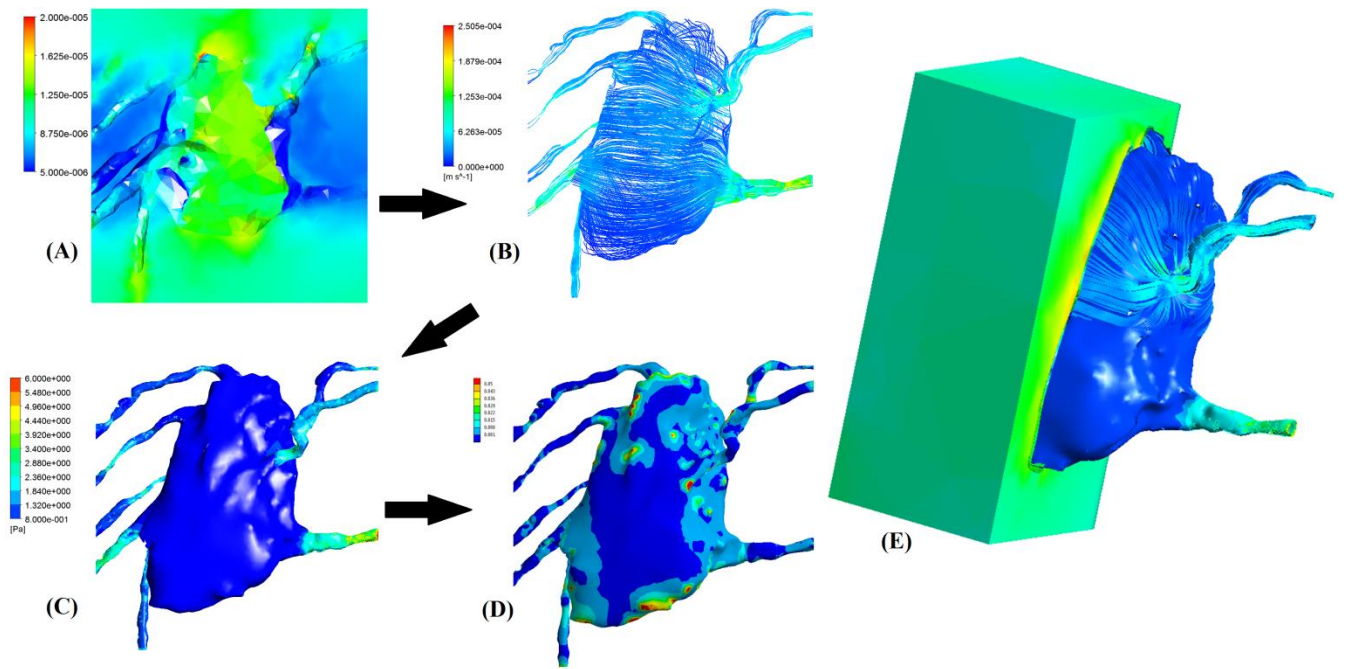
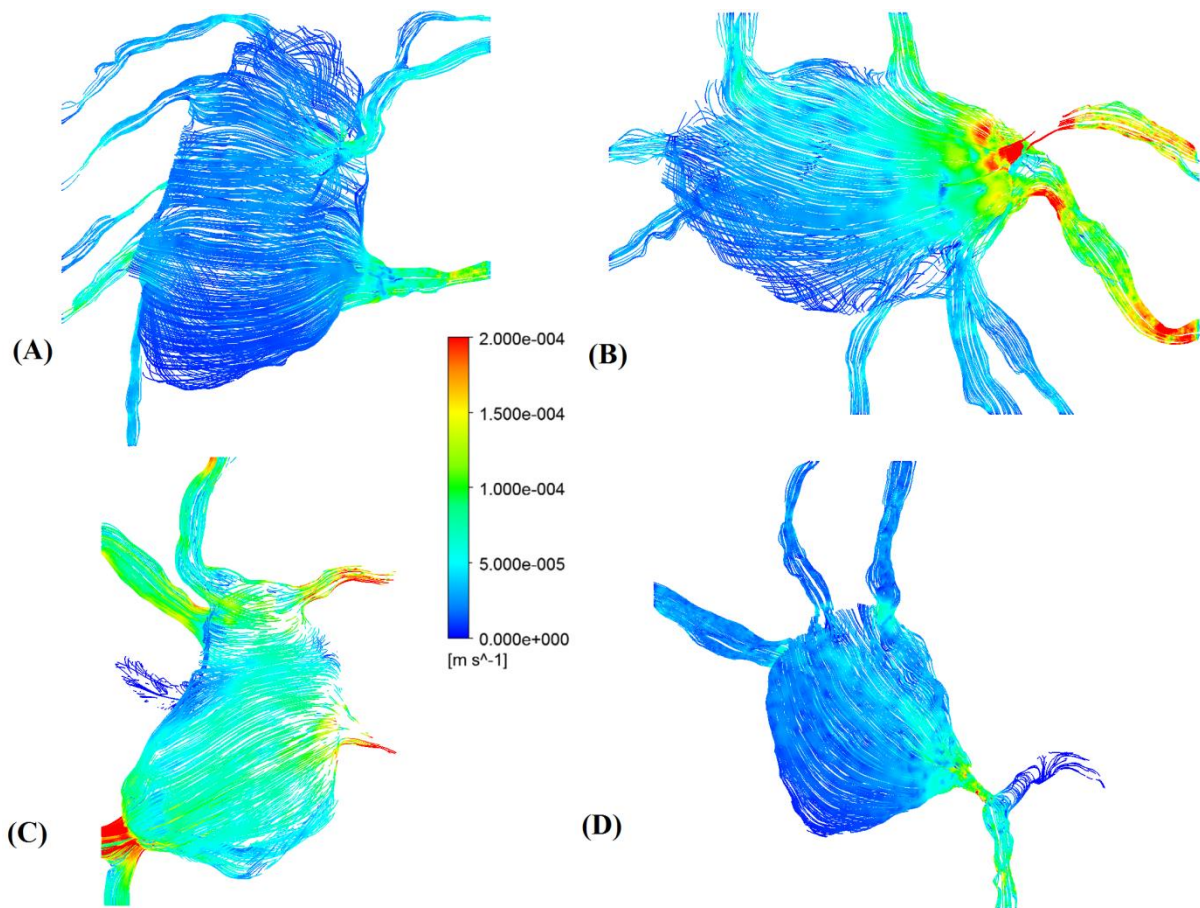


Fig. 2 (A) Strain distribution in the bone matrix around a representative osteocyte, (B) streamlines of the fluid flow within the pericellular space around the osteocyte, (C) shear stress imparted on the cell membrane by the fluid flow and (D) the resulting strain within the osteocyte. A composite image of these contour plots is also shown (E).

1
 2
 3
 4
 5
 6
 7
 8
 9
 10
 11
 12
 13
 14
 15
 16



1
2 **Fig. 3** Images showing velocity streamlines in pericellular space surrounding representative
3 osteocytes
4

5
6
7
8
9
10
11
12

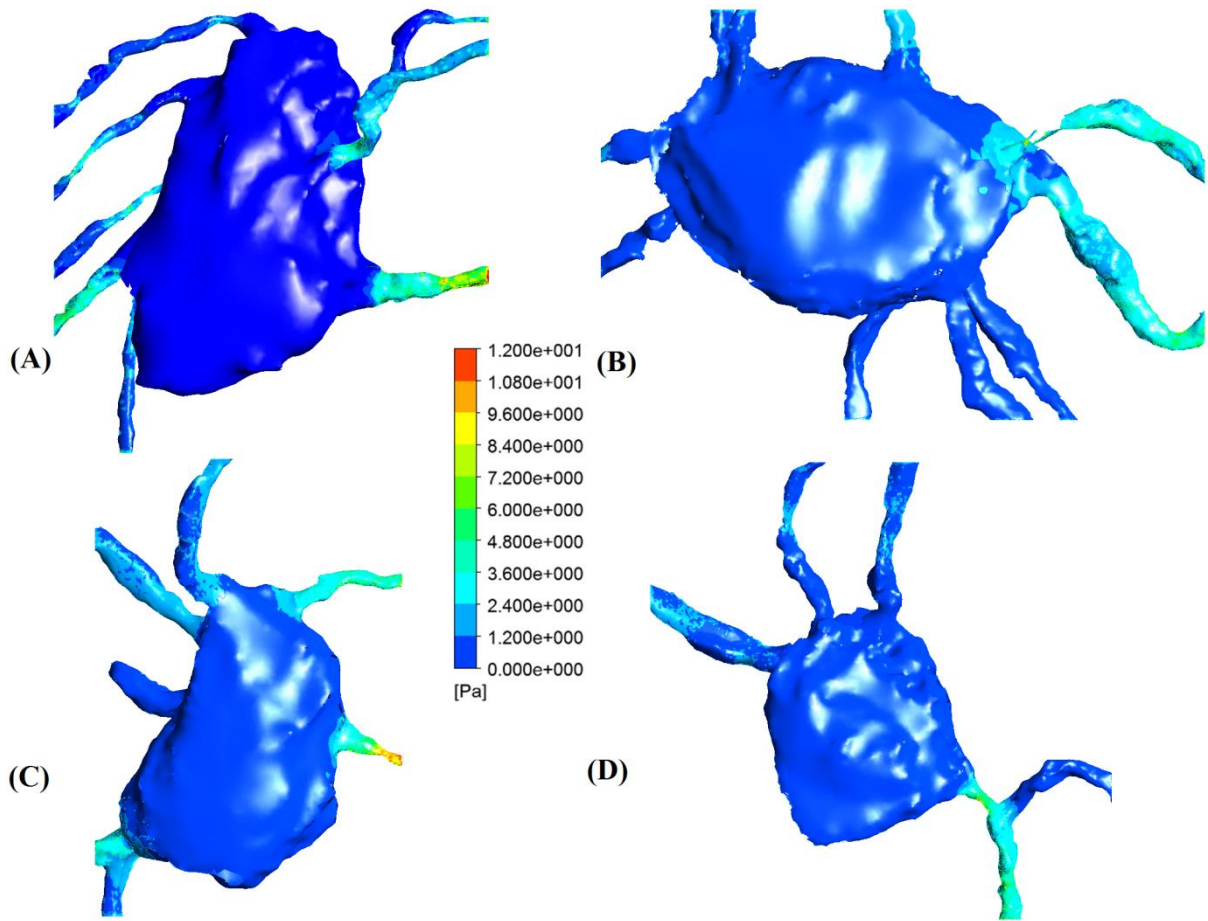


Fig. 4 Images showing contour plots of shear stress on representative osteocyte cell membranes.

1
2
3
4
5
6
7
8
9
10
11
12

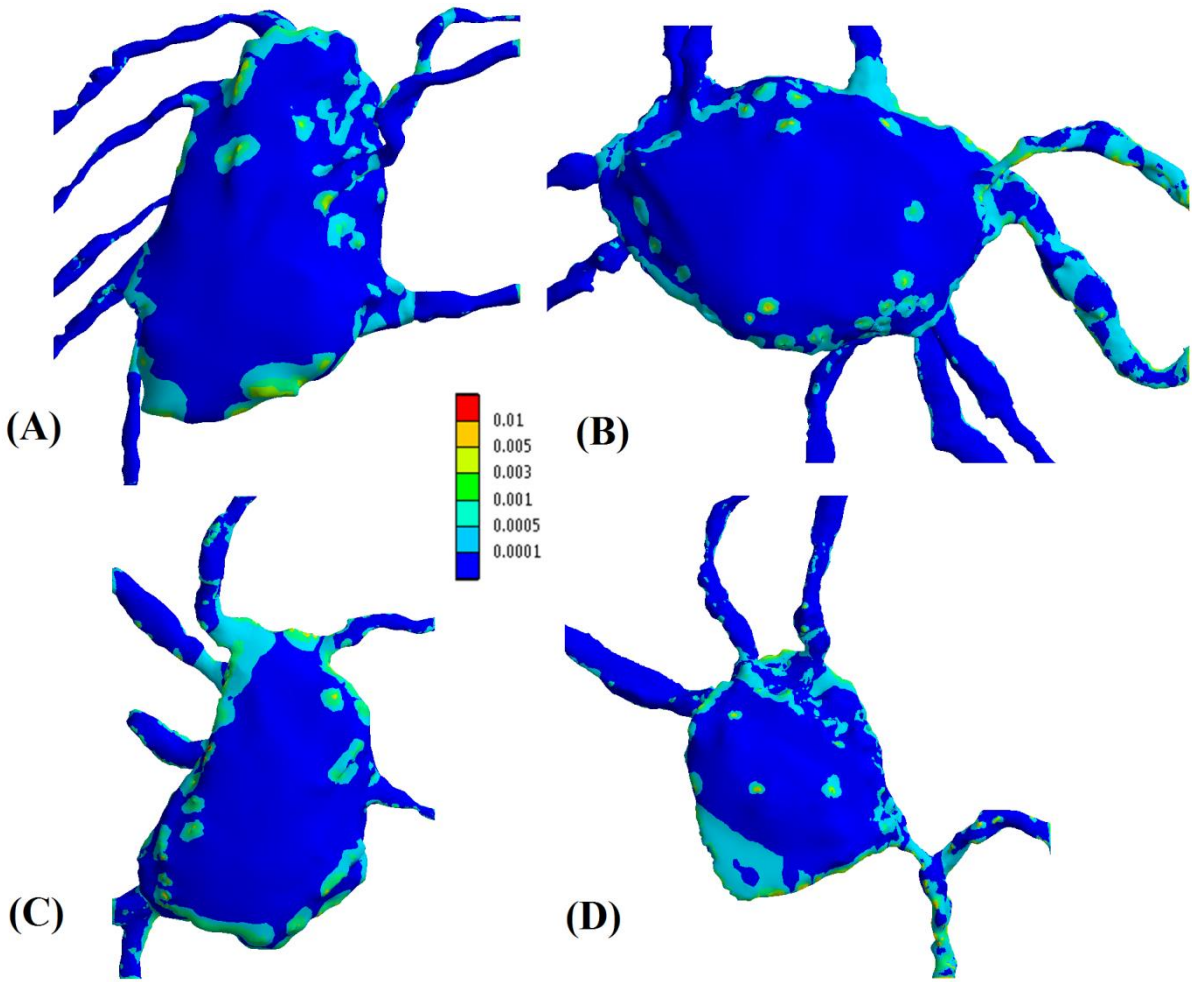
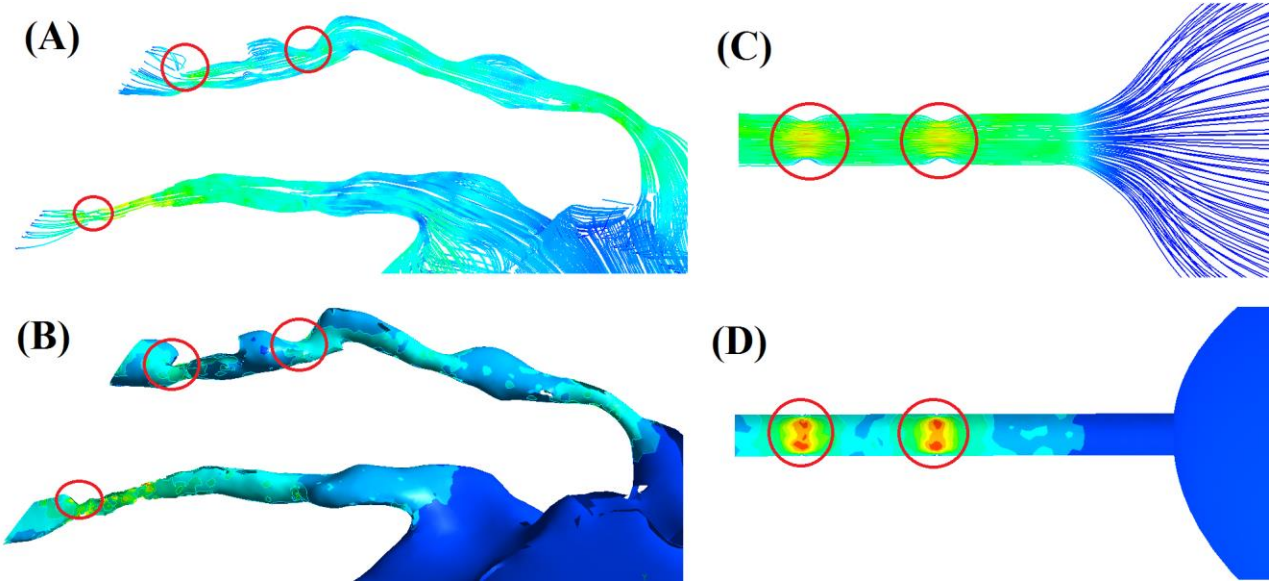


Fig. 5 Contour plots of maximum principal strain distributions in representative osteocyte cell membranes



1
2
3
4
5
6
7
8
9
10
11
12
13

Fig. 6 Contour plots showing the stimulus amplification effect within the canaliculi, with the effect of the ECM projections clearly visible on (A) velocity and (B) shear stress in a representative osteocyte, and similarly on (C) velocity and (D) shear stress in an idealised model.

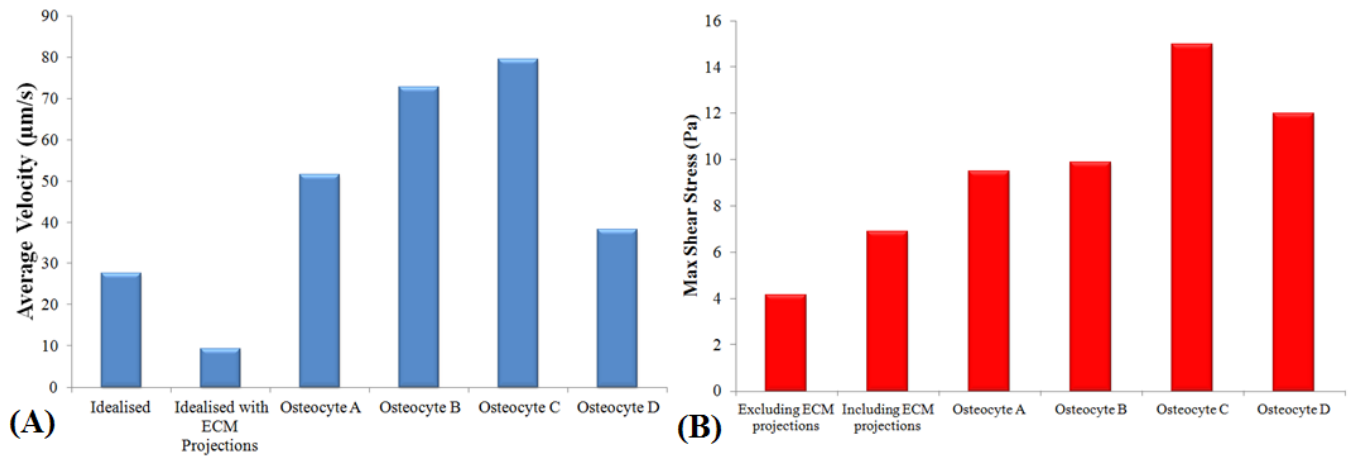
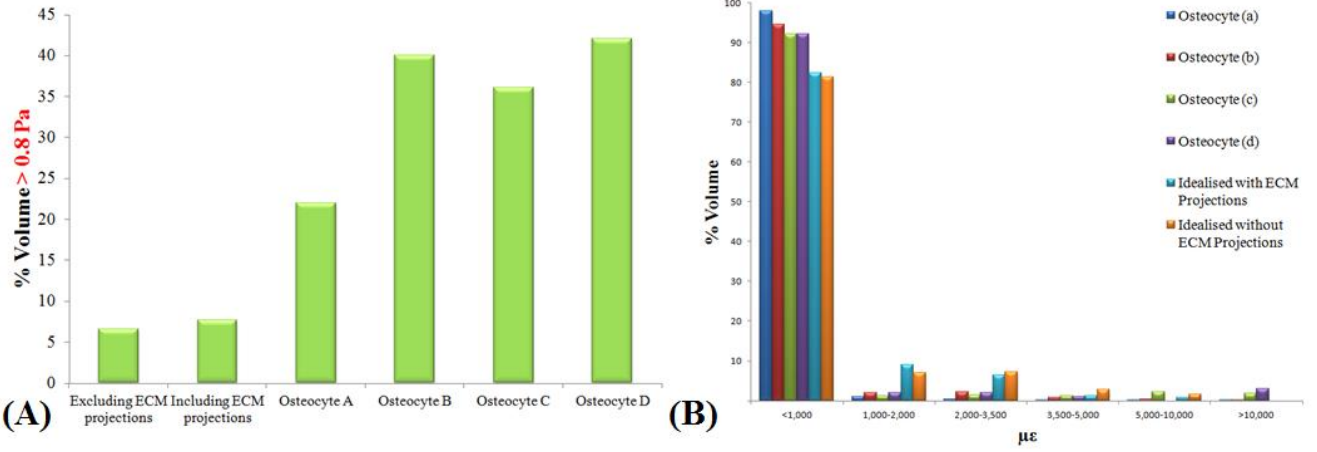


Fig. 7 Average interstitial fluid velocities within the pericellular space in osteocyte models (A) and the resulting maximum shear stresses on the osteocyte cell membranes (B).

1
2
3
4
5
6
7
8
9
10
11
12
13
14
15
16
17
18



1

2

Fig. 8 The percentage of the osteocyte models stimulated above 0.8 Pa (A) and the strain

3

distribution in the osteocytes arising from the mechanically-driven fluid flow (B).